HHS Public Access

Author manuscript

Nat Med. Author manuscript; available in PMC 2019 January 23.

Published in final edited form as:

Nat Med. 2018 September ; 24(9): 1330–1336. doi:10.1038/s41591-018-0117-4.

Cytotoxic CD8+ T cells recognize and kill *Plasmodium vivax*-infected reticulocytes

Caroline Junqueira[1,2,*], **Camila R. R. Barbosa**[1], **Pedro A. C. Costa**[1], **Andréa Teixeira-Carvalho**[1], **Guilherme Castro**[1], **Sumit Sen Santara**[2], **Rafael P. Barbosa**[2], **Farokh Dotiwala**[2], **Dhelio B. Pereira**[3], **Lis R. Antonelli**[1], **Judy Lieberman**[2,*], and **Ricardo T. Gazzinelli**[4,5,6,*]

[1]Laboratório de Imunopatologia, Instituto René Rachou, Fundação Oswaldo Cruz, Belo Horizonte, MG 30190-009, Brazil

[2]Program in Cellular and Molecular Medicine, Boston Children's Hospital and Department of Pediatrics, Harvard Medical School, Boston, MA 02115, USA

[3]Centro de Pesquisas em Medicina Tropical, Porto Velho, RO 76812-329, Brazil

[4]Plataforma de Medicina Translacional, Fundação Oswaldo Cruz, Ribeirão Preto, SP 14049-900, Brazil

[5]Departamento de Bioquímica e Imunologia, Universidade Federal de Minas Gerais, Belo Horizonte, MG 31270-901, Brazil

[6]Division of Infectious Disease and Immunology, University of Massachusetts Medical School, Worcester, MA 01605, USA

Abstract

Plasmodium vivax causes approximately 100 million clinical malaria cases yearly[1,2]. The basis of protective immunity is poorly understood and thought to be mediated by antibodies[3,4]. Cytotoxic $CD8^+$ T cells (CTLs) protect against other intracellular parasites by detecting parasite peptides presented by Human Leukocyte Antigen Class I (HLA-I) on host cells. CTLs kill parasite-infected mammalian cells and intracellular parasites by releasing their cytotoxic granules[5,6]. Perforin (PFN) delivers the antimicrobial peptide granulysin (GNLY) and death-inducing granzymes (Gzm) into the host cell, and GNLY then delivers Gzms into the parasite. CTLs were thought to have no role against *Plasmodium spp*. blood stages because red blood cells (RBCs) generally do not express HLA-I[7]. However, *P. vivax* infects reticulocytes (Retics) that retain the protein translation

*Please address correspondence to: carolinejunqueira@minas.fiocruz.br; judy.lieberman@childrens.harvard.edu; or ricardo.gazzinelli@umassmed.edu.

Correspondence and requests for materials should be addressed to C.J.

Author contributions

C.J., J.L. and R.T.G. conceived; C.J. and R.T.G. supervised this study; D.B.P. recruited the patients and healthy donors; C.J., L.R.A., A.T.-C., J.L. and R.T.G. designed and analyzed experiments; C.J., C.R.R.B., L.R.A., P.A.C.C., A.T.-C., G.C and R.P.B. performed experiments; S.S.S. and F.D. contributed reagents; C.J., C.R.R.B., P.A.C.C. and L.R.A. prepared figures and helped with manuscript preparation; and C.J., J.L. and R.T.G. wrote the paper.

Competing interests

The authors declare no competing financial interests.

machinery. Here we show that *P. vivax*-infected Retics (iRetic) express HLA-I. Infected patient circulating $CD8^+$ T cells highly express cytotoxic proteins and recognize and form immunological synapses with iRetics in an HLA-dependent manner, releasing their cytotoxic granules to kill both host cell and intracellular parasite, preventing reinvasion. iRetic and parasite killing is PFN-independent, but depends on GNLY, which generally efficiently forms pores only in microbial membranes[8]. We find that *P. vivax* depletes cholesterol from the iRetic cell membrane, rendering it GNLY-susceptible. This unexpected T cell defense might be mobilized to improve *P. vivax* vaccine efficacy.

Keywords

$CD8^+$ T cells; CTL; granzyme; granulysin; *Plasmodium*; malaria; reticulocyte

Although less virulent than *P. falciparum*, *P. vivax* can cause life-threatening cerebral malaria, acute respiratory distress syndrome, splenic rupture, hepatitis, severe anemia and thrombocytopenia, and aggravate co-morbidities[9–11]. Both $CD8^+$ T cell IFNγ and cytotoxicity protect against the *Plasmodium* circumsporozoite stages in hepatocytes[12–15], but CTLs have no known role in fighting the blood stage, which is responsible for clinical pathology. Because host cell invasion requires merozoite Duffy Binding Protein (DBP) interaction with Retic Duffy Protein (DP)[16], inducing anti-DBP blocking antibodies is currently the main strategy for an anti-*P. vivax* malaria vaccine[17]. However, anti-DBP vaccines have not been successful in preclinical models and new vaccine approaches are badly needed[3,4].

Although $CD8^+$ T cells were not expected to recognize the blood stage parasite, we analyzed activation markers on circulating $CD8^+CD3^+$ T cells from uncomplicated *P. vivax* malaria patients by flow cytometry (Fig. 1a,b,). These cells were primarily conventional TCRαβ $CD8^+$ T lymphocytes (Supplementary Fig. 1a,b). Although the abundance of circulating $CD8^+$ T cells and other lymphocytes (NK, γδ T cells, NKT cells) that might contribute to malaria immune defense did not differ in patients and healthy donors (HD) from the same endemic region of Brazil (Supplementary Fig. 1c,d), $CD8^+$ T cells from untreated patients had increased expression of CD69 and HLA-DR activation markers and Ki67, a cell proliferation indicator. These markers returned to levels similar to those in HDs 30–40 days after treatment (AT) with chloroquine and primaquine and parasitological cure. Circulating $CD8^+$ T cell expression of cytotoxic granule GzmB, PFN and GNLY was also significantly increased in malaria patients compared to HD from the endemic area (Figs. 1c,d). These results confirm studies suggesting that circulating $CD8^+$ T cells are activated during *P. vivax,* and to a lesser extent *P. falciparum,* infection[18–22]. Acute patient plasma also contained ~6-fold more GNLY than HD plasma by ELISA (Fig. 1e). To identify the source of GNLY, we analyzed innate, innate-like and conventional αβ T cells from HD and acute malaria patients for GNLY expression (Supplementary Fig. 1e). Most $GNLY^+$ circulating lymphocytes in patients were conventional $CD8^+$ T cells (69.7±1.2%). A higher proportion of $GNLY^+$ circulating lymphocytes were conventional $CD8^+$ T cells in patients than HD ($p = 0.03$). Fewer than 10% of the circulating $GNLY^+$ cells were $CD4^+$ T cells, γδ T cells, NK or NKT

cells in either patients or HDs. Thus, conventional $CD8^+$ T cells express most of the GNLY in infected patients.

Based on these data, we hypothesized that $CD8^+$ T cells in *P. vivax* malaria patients might become activated by recognizing iRetics, causing them to degranulate and release GNLY. Although *P. falciparum* infects mature RBCs, asexual *P. vivax* exclusively infects Retics, which retain the translation machinery, endoplasmic reticulum (ER) and Golgi apparatus needed to produce cell surface proteins. An early electron microscopy study suggested that human Retics weakly express HLA-I[7]. More recent transcriptome and proteome analyses indicated that Retics express HLA and proteins involved in antigen presentation[23,24], including the proteasome, TAP transporter and cofactor TAPASIN, and the ER aminopeptidase ERAP1 (Table S1). We therefore used a pan-class I antibody to compare HLA-I expression on the surface of uninfected and iRetics from patients and HD. iRetics were identified by SYBR Green I staining[25], which stains parasite DNA but not Retic RNA (Supplementary Fig. 2). RBCs were gated based on size and granularity and CD235a (glycophorin A) staining (Fig. 2a), and Retics were identified as $CD235a^+$ and $CD71^+$ (transferrin receptor). As expected[24], acute malaria patient RBCs contained ~5-fold more Retics than HD (Fig. 2b). About half of patient Retics stained for HLA-I, compared to ~10% in HD ($p<0.0001$) (Fig. 2c). 50.3 ± 7.0% of circulating Retics from patients were infected (Fig. 2d) and 57.1 ± 7.9% of iRetics expressed HLA-I at levels comparable to that on B lymphocytes (Fig. 2e,f), but did not express HLA-DR (Fig. 2g). In contrast, <20% of uninfected SYBR $Green^-$ Retics from patients expressed HLA-I ($p<0.0001$). Imaging flow cytometry confirmed HLA-I expression selectively on iRetics, compared to HD Retics (Fig. 2h).

Cell surface HLA expression depends on antigenic peptide binding[26]. To confirm that iRetics have the antigen processing machinery, we used density separation to isolate iRetics from 3 infected donors and uninfected Retics from 3 HD (Supplementary Fig. 3a,b) and analyzed their expression of TAP1 by immunoblot. TAP1 was readily detected in iRetics, but not uninfected Retics (Fig 2i). Thus, iRetics selectively express HLA-I and TAP1, suggesting they might present malaria antigens to $CD8^+$ T cells.

Long-term *P. vivax* culture has not been possible, limiting studies of the immune response to blood stage infection. We developed a short-term *in vitro* culture system[19,27,28] that enabled us to study the $CD8^+$ T cell response to iRetics. $CD8^+$ T cells, isolated by immunomagnetic selection from HD or patients, were cultured for 10 hr with autologous, enriched uninfected Retics or iRetics, respectively (Supplementary Fig. 3c). iRetic incubation activated infected donor $CD8^+$ T cells to express CD69 and Ki67 and produce IFNγ (Figs. 3a–c). In contrast, HD $CD8^+$ T cells did not respond to uninfected Retics. Both patient and HD $CD8^+$ T cells were activated by anti-CD3/anti-CD28. Neither patient nor HD $CD4^+$ T cells responded to iRetics (Fig. 3d). Importantly, HLA-I blocking, but not control, antibody[29] prevented iRetic-induced IFNγ production by $CD8^+$ T cells, but did not affect anti-CD3/anti-CD28 activation, which does not require HLA-I (Fig. 3e). Thus, circulating $CD8^+$ T cells in infected patients specifically recognize HLA-I-bound antigens on iRetics.

Imaging flow cytometry was next used to visualize the $CD8^+$ T cell-iRetic interaction, by staining co-cultures for HLA-I, CD235a, CD3, CD8 and TCR (Fig. 3f,g). 10.9±2.2% of circulating $CD8^+$ T cells from 5 malaria donors formed immune synapses in which TCR, CD3 and CD8 on the T cell capped and co-localized with HLA-I on autologous iRetics. By contrast, <1% of HD $CD8^+$ T cells formed synapses with autologous Retics. To examine whether $CD8^+$ T cells lyse iRetics, CFSE-stained infected donor or HD Retics were co-cultured at different ratios with autologous $CD8^+$ T cells, and the persistence of CFSE-stained cells was assessed by flow cytometry 12 hr later (Fig. 3h,i). Infected donor $CD8^+$ T cells significantly reduced the number of iRetics, but HD $CD8^+$ T cells did not affect uninfected Retics, indicating the specificity of iRetic lysis in infected patients. iRetic lysis by autologous patient $CD8^+$ T cells was confirmed by measuring LDH release that increased with more $CD8^+$ T cells (Fig. 3j). Activated $CD8^+$ T cells kill infected cells by cytotoxic granule exocytosis, which can be measured by externalization of LAMP-1 (CD107a)[30]. After incubation with autologous iRetics, but not uninfected RBCs, infected donor $CD8^+$ T cells stained for surface CD107a, indicating that they degranulated (Fig. 3k). Moreover, the numbers of $CD107a^+CD8^+$ T cells after iRetic co-culture was not significantly different from the numbers that degranulated after anti-CD3/anti-CD28 treatment, suggesting that most of the circulating activated $CD8^+$ CTLs in infected donors specifically recognize iRetics.

CTLs kill other intracellular parasites in a PFN, GNLY and Gzm-dependent manner[5]. To determine how iRetics are lysed and whether *P. vivax* are killed in the process, we first used imaging flow cytometry to determine whether AlexaFlour-488 (AF488)-labeled GNLY and/or GzmB bound and/or entered uninfected Retics or iRetics (Fig. 4a–f). GNLY, but not GzmB on its own, selectively bound to iRetics, but not uninfected Retics (Fig. 4a–d). Moreover, when GNLY was present, virtually all iRetics, but not uninfected Retics, stained with GzmB (Fig. 4e,f). GNLY co-localized with CD235a on the iRetic membrane, while GzmB was internalized and co-localized with intracellular *P. vivax*, stained with a Hoechst DNA dye (Fig. 4g, Supplementary Fig. 4). In some iRetic, GzmB also showed punctate host cell staining, which might represent GzmB trafficking to host mitochondria, where Gzms concentrate[31]. Thus, GNLY, independently of PFN, delivers GzmB to the parasite, a surprising finding, since in other intracellular parasite infections, PFN is required to deliver GNLY and Gzms across host cell membranes[5].

GNLY permeabilizes cholesterol-containing mammalian cell membranes only at exceedingly high (micromolar) concentrations, since cholesterol inhibits pore formation[8]. In contrast, PFN is a cholesterol-dependent cytolysin. Other *Plasmodium* species harvest and deplete cholesterol from RBC membranes[32,33], which could make them susceptible to GNLY. When we depleted cholesterol from RBC membranes using methyl-β-cyclodextrin (mβCD), AF488-labeled GNLY attached to the cholesterol-depleted, but not to untreated, RBC membranes (Fig. 4h), delivered GzmB-AF488 into the RBC (Fig. 4i), and lysed cholesterol-depleted RBCs (Fig. 4j). To determine whether cholesterol was depleted from iRetic membranes, we stained Retics with 25-[N-[(7-nitro-2-1,3-benzoxadiazol-4-yl)methyl]amino]-27-norcholesterol (25-NBD-cholesterol), a fluorescent cholesterol mimic. iRetics, but not uninfected Retics, stained brightly with 25-NBD-cholesterol (Fig. 4k,l),

suggesting that *P. vivax* also harvests cholesterol from iRetic membranes, making them GNLY-susceptible.

GNLY-delivered GzmB co-localization with the parasite (Fig. 4g) suggested that GNLY and GzmB would not only lyse iRetics, but might also directly kill the parasite. To determine which cytotoxic molecules are required to lyse iRetics and whether intracellular parasites are also killed, we incubated GNLY, GzmB and/or PFN with iRetics (Fig. 4m) or HD uninfected Retics (Fig. 4n) for 1 hr and measured RBC lysis by LDH release and parasite viability by the ability to invade fresh Retics[34] (Fig. 4o). GNLY on its own lysed iRetics, but GzmB or PFN, alone or together, had no significant effect. However, GNLY and GzmB was significantly more cytotoxic than GNLY, and GzmB, GNLY and PFN further significantly enhanced iRetic lysis. Importantly, uninfected Retics were unaffected by GzmB or GNLY, but were lysed by PFN, as expected, because their membranes are cholesterol-rich. GNLY alone inhibited parasite invasion of fresh RBC, but GNLY and GzmB together or all three cytotoxic molecules completely blocked reinvasion. Reinvasion could be inhibited because of parasite killing or because parasite maturation or infectious merozoite release was hindered. To determine whether the parasites within iRetics were directly damaged, we analyzed iRetic morphology by electron microscopy after treatment with GNLY±GzmB (Fig. 4o). After just GNLY, the treated iRetics swelled and the intracellular parasites started to show signs of death, such as cytoplasmic vacuolization, consistent with iRetic membrane damage by GNLY. However, after incubation with both GNLY and GzmB, intracellular parasites developed swollen and fragmented mitochondria, condensed nuclei, and cytoplasmic vacuolization, and the parasitophorous vacuole membrane was disrupted (Fig. 4p). These changes resembled morphological changes seen after GzmB and GNLY treatment of other protozoan parasites[5]. The protocol used to select iRetics enriches for trophozoite stage infection. Thus, GNLY and GzmB not only lyse iRetic, but also directly kill intracellular trophozoites and block reinvasion.

In conclusion, *P. vivax* iRetics highly express HLA-I and are specifically recognized by $CD8^+$ T cells. This is, to our knowledge, a unique example of $CD8^+$ T cells recognizing Retics in an HLA-restricted antigen-specific manner. Because GNLY on its own delivers GzmB into iRetics, the CTL mechanism that lyses iRetics is distinct from granule-mediated killing of other mammalian target cells and intracellular parasites, which requires PFN. iRetic lysis would be expected to reduce parasite infectivity by releasing parasites that have not yet matured to the infectious merozoite stage from their obligate intracellular niche. However, here we provide evidence that $CD8^+$ T cells also directly kill *P. vivax*, which should enhance immune effectiveness by limiting spreading of infectious organisms. Although patient CTLs lysed iRetics in a 12 hr assay, parasite killing and inhibition of reinvasion occurred within an hour of adding GNLY and GzmB, suggesting that parasite death is rapid. The molecular mechanism of *P. vivax* killing remains to be defined, which will be challenging without long-term culture systems for *P. vivax*. Nevertheless, our findings identify a previously unsuspected protective mechanism against blood stage parasites and suggest that a vaccine that elicits CTLs against blood stage *P. vivax* may help prevent transmission and control disease severity. In the future, it will be worthwhile to examine whether other innate or innate-like killer lymphocytes that express GNLY, such as NK and γδ T cells, recognize and kill iRetic and play a role in immune protection[35–39].

Future studies are also needed to determine whether killer lymphocytes are always beneficial during blood stage malaria, since they might contribute to anemia, inflammation or other pathological sequelae of infection.

Methods

Malaria patients and healthy donors

Male and female healthy donors (HD) and *P. vivax*-infected patients, aged 18–60, were recruited from the Amazon malaria endemic area from the outpatient malaria clinic in the Tropical Medicine Research Center in Porto Velho, Brazil, with informed consent using a protocol approved by the Institutional Review Boards of the Oswaldo Cruz Foundation and National Ethical Council (CAAE: 59902816.7.0000.5091), University of Massachusetts Medical School (11116) and Boston Children's Hospital (00005698). The exclusion criteria were co-infection with *P. falciparum,* chronic inflammatory or infectious diseases or pregnancy. Infected patients were clinically evaluated and tested for *Plasmodium* infection by thick smear and PCR during symptomatic stage and 40 days after treatment with chloroquine and primaquine. All relevant ethical regulations were followed while conducting this work.

Reagents

All antibodies and fluorescent dies used in our experiments are listed on Table S2.

Sample preparation

PBMCs, obtained by Ficoll (GE Healthcare, USA) gradient centrifugation as previous described[40], were stained for CD69, Ki67, HLA-DR, PFN, GNLY and GzmB. $CD8^+$ and $CD4^+$ T cells were purified from PBMCs by positive selection using Dynabeads (ThermoFisher Scientific). The RBC pellet, suspended in isotonic Percoll, was used to purify iRetics from malaria patient samples on a 45% isotonic Percoll (GE Healthcare, USA) gradient and uRetics from HD on 70% Percoll. Uninfected erythrocytes (uRBCs) were obtained from the Percoll gradient pellet.

T lymphocyte and RBC coculture

Purified T cells (10^5/well) and Retics (5×10^5/well) were co-cultured at 37°C for 10 hr in 96-well plates to assess T cell activation, IFNγ production and degranulation (CD107a)[41]. Some experiments were performed in the presence of 2 μg/ml HLA-ABC blocking antibody (W6/33) or isotype control, which were added to $CD8^+$ T cells 30 min before RBC coculture. T lymphocytes cultured with 1 μg/ml anti-CD3 (BD Pharmingen) and 0.5 μg/ml anti-CD28 (BD Pharmingen) were used as positive controls.

Flow cytometry

T cell surface were stained with anti-CD4, anti-CD8, anti-CD3, anti-CD69, anti-HLA-DR, anti-Ki67, anti-CD19, anti-γδ TCR, anti-αβ TCR, anti-CD56, anti-CD161 and anti-TCRVα7.2. RBCs were stained with anti-CD71, anti-CD235a, anti-HLA-ABC (class I), anti-HLA-DR (class II), Thiazole Orange and SYBR Green I (*P. vivax* DNA)[25,42–44]. To

analyze intracellular cytokine and granule protein expression, cells were incubated at 37°C, 5% CO_2 in the presence of indicated stimuli for 30 min before adding Brefeldin A (1μl/ml) and Monensin (1μl/ml) (BD Pharmingen) solutions and culture for an additional 4–10 hr prior to staining. Cells were first stained for indicated cell surface markers, then permeabilized in Fix/Perm buffer, and stained in Perm/Wash buffer (BD Pharmingen) for IFNγ or cytotoxic granule proteins as per the manufacturer's instructions. Flow cytometry was performed using a FACScan flow cytometer (Becton Dickinson, USA), Fortessa (Becton Dickinson, USA) or Celesta (Becton Dickinson, USA) and analyzed using FlowJo software V.10 (Tri-Star, USA).

Plasma granulysin

GNLY in plasma from healthy donors and *P. vivax*-infected patients was measured using the Human Granulysin DuoSet ELISA (R&D Systems, USA).

Reticulocyte protein expression

Cell lysates of iRetics and HD uRetics, obtained by lysis in RIPA buffer (Sigma-Aldrich) in the presence of complete protease inhibitor (Roche, CH), were analyzed by immunoblot probed for TAP1 after hemoglobin removal using HemogloBind (Biotech Support Group, USA). Each retic lane was loaded with 50 μg protein, while PBMC control sample contained 20 μg protein. The same membrane was probed for β-actin and F-actin as loading controls. β-actin was used as loading control for HD uRetics and F-actin for iRetics because host cell remodeling of the actin cytoskeleton under *Plasmodium* infection[45,46]. The secondary anti-mouse or anti-rabbit IgG antibody was detected by chemiluminescence.

Proteomic and transcriptomic analysis

Databases for the Retic proteome[23] and transcriptome[24] were analyzed for expression of proteins involved in the endogenous antigen presentation pathway (Table S1) using ID_REF data deposited in the Gene Expression Omnibus (http://www.ncbi.nlm.nih.gov/geo/) (accession numbers: GSM143572–143599, GSM143671–143682, GSM143703, GSM143706–143716, GSM143718–143721).

Cytotoxic enzymes

GzmB, GNLY and PFN were purified from YT-Indy cells as described[46]. Purity was >95%, as determined by Coomassie stained SDS-PAGE. Protein concentrations were determined by Bradford assay. Specific activity of GNLY and PFN was determined by serial dilution on infected and uninfected reticulocytes; a sublytic concentration (<20% killing, adequate to deliver Gzms, but not kill most host cells) was used in all experiments. Specific activity of GzmB was determined by cleavage of the peptide substrate, t-Butyloxycarbonyl-Ala-Ala-Asp-ThioBenzyl ester (Boc-AAD-SBzl), in the presence of 5,5′Dithio-bis (2-nitrobenzoic acid) (DTNB).

Reticulocyte lysis assay

iRetics labeled with carboxyfluorescein diacetate succinimidyl ester (CFSE, Sigma-Aldrich) were cultured with $CD8^+$ T cells at indicated ratios. Twelve hours later, cells were harvested

and stained for CD235a and CD8. The number of surviving $CFSE^+$ gated $CD235a^+$ cells was compared with the number of $CFSE^+$ cells surviving after culture in the absence of lymphocytes. Lactate dehydrogenase (LDH) release, measured by CytoTox 96 (Promega, USA), was used to assess RBC lysis after co-culture for 12 hr with $CD8^+$ T cells at indicated E:T ratios. To assess cytolysis by purified granule proteins, iRetics were incubated for 1 hr at 37°C with 100 nM GNLY ± 500 nM GzmB ± a sublytic concentration of PFN and the culture supernatants were analyzed by LDH release assay. The morphology of treated Retics was assessed by electron microscopy.

Parasite invasion assay

Invasion assays were performed as previously described[47]. Infected reticulocytes from *P. vivax* malaria patients, enriched on a 45% Percoll gradient, were treated with 100 nM GNLY ± 500 nM GzmB ± a sublytic concentration of PFN for 1 hr at 37°C. Uninfected HD reticulocytes, obtained from a 70% Percoll gradient, were added to the washed, treated iRetics at a ratio of 10:1. After 24 hr coculture, cytospins were stained with Giemsa and the proportion of newly invaded ring stage-infected cells was enumerated.

Imaging flow cytometry

Purified $CD8^+$ T cells and Retics were co-cultured at an E:T ratio of 1:5 for 1 hr and then stained with HLA-ABC, TCR, CD3, CD8 and CD235a antibodies before analysis on an ImageStream Amnis X using Ideas software (Amnis, USA). $CD235a^+CD3^+$ doublets were selected based on aspect ratio versus cell area. Purified iRetics and uRetics were incubated with 100 nM GNLY-Alexa Fluor 488 or 500 nM GzmB-Alexa Fluor 488 in the presence or absence of 100 nM unlabeled GNLY for 1 hr at 37°C as described[1]. Cells were washed and fixed with 2% PFA in PBS prior to imaging flow cytometry. The frequency of cells staining for GNLY and GzmB was quantified using Ideas software. To analyze colocalization, images of iRetics incubated for 1 hr with 100 nM GNLY-Alexa Fluor 647 and 500 nM GzmB-Alexa Fluor 488 were stained with CD235a-PE and Hoechst 33342.

Cholesterol depletion

HD RBCs in HBSS were untreated or incubated with indicated concentrations of methyl-beta-cyclodextrin for 30 min at 37°C before adding indicated amounts of purified GNLY and GzmB or GzmB-Alexa Fluor 488 and culturing for 1 h. Treated cells were analyzed by flow cytometry for GNLY and GzmB uptake by flow cytometry or for LDH release as above.

Electron Microscopy

Purified iRetics incubated with 100 nM GNLY ± 500 nM GzmB were fixed in 2.5% buffered glutaraldehyde solution, 0.1 M, pH 7.2, for 3 hr at 4°C, washed and the cell pellet was immersed in 4% agarose. The pellet was fixed in 1% osmium tetroxide and 1.5% (w/v) potassium ferrocyanide, dehydrated in ethanol and embedded in Araldite 502 (Electron Microscopy Sciences, Hatfield, PA, USA). Extra thin sections, obtained using a Sorvall MT-2B ultramicrotome (Dupont, USA), were applied to 200-mesh copper grids (Ted Pella, USA) and stained with 2% uranyl acetate and Reynolds' lead citrate. Images were obtained

by transmission electron microscopy using a Tecnai G2-12 - SpiritBiotwin FEI -120 kV (FEI, JP).

Statistical Analysis

Statistical analysis was performed using GraphPad Prism V7.0. Prior to applying statistical methods, whether the data fit a normal distribution was evaluated by the D'Agostino and Pearson normality test. The distribution was considered normal when $p \leq 0.05$. Parametric or non-parametric (Mann-Whitney test) two-tailed paired and unpaired *t*-tests were used to compare two groups at 95% confidence interval (CI). Multiple groups were compared by two-way ANOVA with additional Tukey's multiple comparisons test at 95% CI. Simple column comparisons were analyzed by one-way ANOVA using the Kruskal-Wallis test and Tukey's multiple comparisons test at 95% CI. Differences were considered statistically significant when $p \leq 0.05$. All the p values less them 0.0001 are shown as $p < 0.0001$.

Supplementary Material

Refer to Web version on PubMed Central for supplementary material.

Acknowledgments

We thank Dr. Kasturi Haldar and Kenneth Rock for scientific discussions and suggestions during the development of this work. We are grateful to the Program for Technological Development in Tools for Health–PDTIS-FIOCRUZ for use of its facilities; and to the clinic, laboratory and administrative staff as well as field workers and subjects from Porto Velho who participated in the study. This study was funded by the National Institutes of Health (1R01NS098747 to R.T.G.; the Amazonian-ICEMR U19 AI089681 to C.J., L.R.A. and R.T.G.; 1R01AI116577 and R21AI131632-01 to R.T.G and J.L.); National Institute of Science and Technology for Vaccines/Conselho Nacional de Desenvolvimento Científico e Tecnológico (465293/2014-0 to C.J., L.R.A., D.B.P. and R.T.G.) and Fundação de Amparo à Pesquisa do Estado de Minas Gerais (RED-00012-14 and APQ-00653-16 to C.J. and R.T.G.); and Fundação de Amparo à Pesquisa do Estado de São Paulo (2016/23618-8 to R.T.G.). C.J., L.R.A., A.T.C. and R.T.G. are recipients of CNPq fellowships; P.A.C. and C.R.B. are fellows from FAPEMIG; and C.J. is a fellow from Coordenação de Aperfeiçoamento de Pessoal de Ensino Superior (CAPES).

References

1. Anstey NM, Douglas NM, Poespoprodjo JR, Price RN. Plasmodium vivax: clinical spectrum, risk factors and pathogenesis. Adv Parasitol. 2012; 80:151–201. [PubMed: 23199488]
2. Miller LH, Ackerman HC, Su XZ, Wellems TE. Malaria biology and disease pathogenesis: insights for new treatments. Nat Med. 2013; 19:156–167. [PubMed: 23389616]
3. Zimmerman PA, Ferreira MU, Howes RE, Mercereau-Puijalon O. Red blood cell polymorphism and susceptibility to Plasmodium vivax. Adv Parasitol. 2013; 81:27–76. [PubMed: 23384621]
4. Mueller I, Shakri AR, Chitnis CE. Development of vaccines for Plasmodium vivax malaria. Vaccine. 2015; 33:7489–7495. [PubMed: 26428453]
5. Dotiwala F, et al. Killer lymphocytes use granulysin, perforin and granzymes to kill intracellular parasites. Nat Med. 2016; 22:210–216. [PubMed: 26752517]
6. Walch M, et al. Cytotoxic cells kill intracellular bacteria through granulysin-mediated delivery of granzymes. Cell. 2014; 157:1309–1323. [PubMed: 24906149]
7. Silvestre D, Kourilsky FM, Nicolai MG, Levy JP. Presence of HLA antigens on human reticulocytes as demonstrated by electron microscopy. Nature. 1970; 228:67–68. [PubMed: 5460343]
8. Barman H, et al. Cholesterol in negatively charged lipid bilayers modulates the effect of the antimicrobial protein granulysin. J Membr Biol. 2006; 212:29–39. [PubMed: 17206515]
9. Bassat Q, Alonso PL. Defying malaria: Fathoming severe Plasmodium vivax disease. Nat Med. 2011; 17:48–49. [PubMed: 21217683]

10. Murray CJ, et al. Global malaria mortality between 1980 and 2010: a systematic analysis. Lancet. 2012; 379:413–431. [PubMed: 22305225]
11. Lacerda MV, et al. Understanding the clinical spectrum of complicated Plasmodium vivax malaria: a systematic review on the contributions of the Brazilian literature. Malar J. 2012; 11:12. [PubMed: 22230294]
12. Chakravarty S, Baldeviano GC, Overstreet MG, Zavala F. Effector CD8+ T lymphocytes against liver stages of Plasmodium yoelii do not require gamma interferon for antiparasite activity. Infect Immun. 2008; 76:3628–3631. [PubMed: 18519561]
13. Spencer AJ, et al. The Threshold of Protection from Liver-Stage Malaria Relies on a Fine Balance between the Number of Infected Hepatocytes and Effector CD8(+) T Cells Present in the Liver. J Immunol. 2017; 198:2006–2016. [PubMed: 28087668]
14. Schofield L, et al. Gamma interferon, CD8+ T cells and antibodies required for immunity to malaria sporozoites. Nature. 1987; 330:664–666. [PubMed: 3120015]
15. Seguin MC, et al. Induction of nitric oxide synthase protects against malaria in mice exposed to irradiated Plasmodium berghei infected mosquitoes: involvement of interferon gamma and CD8+ T cells. J Exp Med. 1994; 180:353–358. [PubMed: 7516412]
16. Miller LH, Mason SJ, Dvorak JA, McGinniss MH, Rothman IK. Erythrocyte receptors for (Plasmodium knowlesi) malaria: Duffy blood group determinants. Science. 1975; 189:561–563. [PubMed: 1145213]
17. King CL, et al. Naturally acquired Duffy-binding protein-specific binding inhibitory antibodies confer protection from blood-stage Plasmodium vivax infection. Proc Natl Acad Sci U S A. 2008; 105:8363–8368. [PubMed: 18523022]
18. Safeukui I, et al. Malaria induces anemia through CD8+ T cell-dependent parasite clearance and erythrocyte removal in the spleen. MBio. 2015; 6
19. Costa PA, et al. Induction of Inhibitory Receptors on T Cells During Plasmodium vivax Malaria Impairs Cytokine Production. J Infect Dis. 2015; 212:1999–2010. [PubMed: 26019284]
20. Hojo-Souza NS, et al. Phenotypic profiling of CD8(+) T cells during Plasmodium vivax blood-stage infection. BMC Infect Dis. 2015; 15:35. [PubMed: 25636730]
21. Burel JG, Apte SH, McCarthy JS, Doolan DL. Plasmodium vivax but Not Plasmodium falciparum Blood-Stage Infection in Humans Is Associated with the Expansion of a CD8+ T Cell Population with Cytotoxic Potential. PLoS Negl Trop Dis. 2016; 10:e0005031. [PubMed: 27930660]
22. Falanga YT, et al. High pathogen burden in childhood promotes the development of unconventional innate-like CD8+ T cells. JCI Insight. 2017; 2
23. Wilson MC, et al. Comparison of the Proteome of Adult and Cord Erythroid Cells, and Changes in the Proteome Following Reticulocyte Maturation. Mol Cell Proteomics. 2016; 15:1938–1946. [PubMed: 27006477]
24. Goh SH, et al. The human reticulocyte transcriptome. Physiol Genomics. 2007; 30:172–178. [PubMed: 17405831]
25. Malleret B, et al. A rapid and robust tri-color flow cytometry assay for monitoring malaria parasite development. Sci Rep. 2011; 1:118. [PubMed: 22355635]
26. Hoffmann JJ, Pennings JM. Pseudo-reticulocytosis as a result of malaria parasites. Clin Lab Haematol. 1999; 21:257–260. [PubMed: 10583327]
27. Raghavan M, Del Cid N, Rizvi SM, Peters LR. MHC class I assembly: out and about. Trends Immunol. 2008; 29:436–443. [PubMed: 18675588]
28. Antonelli LR, et al. The CD14+CD16+ inflammatory monocyte subset displays increased mitochondrial activity and effector function during acute Plasmodium vivax malaria. PLoS Pathog. 2014; 10:e1004393. [PubMed: 25233271]
29. Rocha BC, et al. Type I Interferon Transcriptional Signature in Neutrophils and Low-Density Granulocytes Are Associated with Tissue Damage in Malaria. Cell Rep. 2015; 13:2829–2841. [PubMed: 26711347]
30. Heemskerk MH, et al. Dual HLA class I and class II restricted recognition of alloreactive T lymphocytes mediated by a single T cell receptor complex. Proc Natl Acad Sci U S A. 2001; 98:6806–6811. [PubMed: 11381117]

31. Martinvalet D, Dykxhoorn DM, Ferrini R, Lieberman J. Granzyme A cleaves a mitochondrial complex I protein to initiate caspase-independent cell death. Cell. 2008; 133:681–692. [PubMed: 18485875]
32. Lauer S, et al. Vacuolar uptake of host components, and a role for cholesterol and sphingomyelin in malarial infection. EMBO J. 2000; 19:3556–3564. [PubMed: 10899110]
33. Holz GG Jr. Lipids and the malarial parasite. Bull World Health Organ. 1977; 55:237–248. [PubMed: 412602]
34. Russell B, et al. A reliable ex vivo invasion assay of human reticulocytes by Plasmodium vivax. Blood. 2011; 118:e74–81. [PubMed: 21768300]
35. Ramsey JM, et al. Plasmodium falciparum and P. vivax gametocyte-specific exoantigens stimulate proliferation of TCR gammadelta+ lymphocytes. J Parasitol. 2002; 88:59–68. [PubMed: 12053981]
36. Artavanis-Tsakonas K, Riley EM. Innate immune response to malaria: rapid induction of IFN-gamma from human NK cells by live Plasmodium falciparum-infected erythrocytes. J Immunol. 2002; 169:2956–2963. [PubMed: 12218109]
37. Artavanis-Tsakonas K, et al. Activation of a subset of human NK cells upon contact with Plasmodium falciparum-infected erythrocytes. J Immunol. 2003; 171:5396–5405. [PubMed: 14607943]
38. Costa G, et al. Control of Plasmodium falciparum erythrocytic cycle: gammadelta T cells target the red blood cell-invasive merozoites. Blood. 2011; 118:6952–6962. [PubMed: 22045985]
39. Troye-Blomberg M, et al. Human gamma delta T cells that inhibit the in vitro growth of the asexual blood stages of the Plasmodium falciparum parasite express cytolytic and proinflammatory molecules. Scand J Immunol. 1999; 50:642–650. [PubMed: 10607313]
40. Boyum A. Isolation of mononuclear cells and granulocytes from human blood. Isolation of monuclear cells by one centrifugation, and of granulocytes by combining centrifugation and sedimentation at 1 g. Scand J Clin Lab Invest Suppl. 1968; 97:77–89. [PubMed: 4179068]
41. Betts MR, et al. Sensitive and viable identification of antigen-specific CD8+ T cells by a flow cytometric assay for degranulation. J Immunol Methods. 2003; 281:65–78. [PubMed: 14580882]
42. Cho JS, et al. Unambiguous determination of Plasmodium vivax reticulocyte invasion by flow cytometry. Int J Parasitol. 2016; 46:31–39. [PubMed: 26385436]
43. Russell B, et al. Field-based flow cytometry for ex vivo characterization of Plasmodium vivax and P. falciparum antimalarial sensitivity. Antimicrob Agents Chemother. 2013; 57:5170–5174. [PubMed: 23877705]
44. Wirjanata G, et al. Quantification of Plasmodium ex vivo drug susceptibility by flow cytometry. Malar J. 2015; 14:417. [PubMed: 26498665]
45. Rug M, et al. Export of virulence proteins by malaria-infected erythrocytes involves remodeling of host actin cytoskeleton. Blood. 2014; 124:3459–3468. [PubMed: 25139348]
46. Cyrklaff M, et al. Hemoglobins S and C interfere with actin remodeling in Plasmodium falciparum-infected erythrocytes. Science. 2011; 334:1283–1286. [PubMed: 22075726]
47. Thiery J, Walch M, Jensen DK, Martinvalet D, Lieberman J. Isolation of cytotoxic T cell and NK granules and purification of their effector proteins. Curr Protoc Cell Biol. 2010; Chapter 3(Unit3): 37.

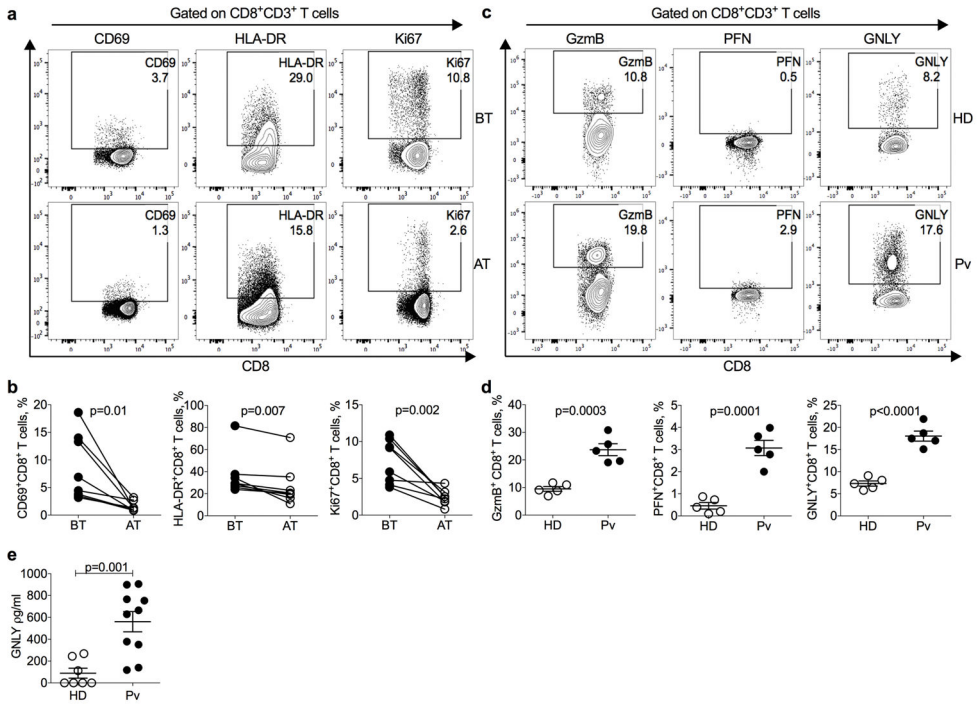

Figure 1. Increased frequency of activated CD8$^+$ T cells in the peripheral blood of *P. vivax* patients

Peripheral blood mononuclear cells (PBMCs) from healthy donors (HD) and *P. vivax* malaria patients (Pv) were gated on CD8$^+$CD3$^+$ T cells (gating strategy described in Supplementary Fig. 1) and analyzed for expression of activation markers and cytotoxic granule proteins by flow cytometry. **a,b,** Shown are representative flow plots (**a**) and the proportion of CD8$^+$ T cells expressing CD69, HLA-DR and Ki67 (**b**) malaria patients, before treatment (BT) and 30–40 days after treatment and parasitological cure (AT). n=8 biologically independent samples/independent experiments. Statistical analysis was performed by two-tailed parametric paired *t*-test at 95% confidence interval (CI). **c,d,** Shown are representative flow plots (**c**) and the proportion of peripheral blood CD8$^+$ T cells expressing GzmB, PFN, and GNLY (**d**) HD and *P. vivax* (Pv) malaria patients BT. n=5 biologically independent samples/independent experiments. **e,** The levels of soluble GNLY in plasma of n=7 HD and n=10 Pv patients BT were measured by ELISA as biologically independent samples/independent experiments. (**d,e)** show mean ± SEM; statistical analysis was performed by two-tailed non-parametric unpaired *t*-test at 95% CI.

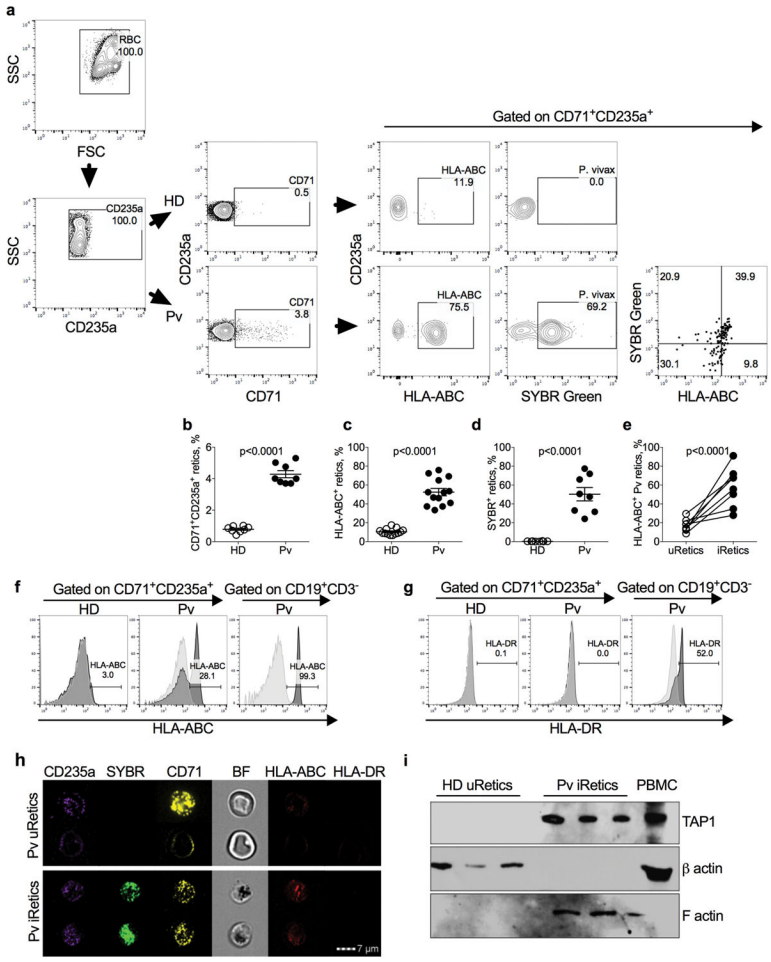

Figure 2. Increased HLA-ABC in *P. vivax* infected reticulocytes

a, Gating strategy to evaluate *P. vivax* infection and HLA-expression in reticulocytes. Top and bottom panels are representative results from a healthy donor (HD) and *P. vivax* acute malaria patient (Pv) before treatment (BT), respectively. Retics are $CD71^+CD235a^+$ and SYBR Green detects parasite DNA in iRetics. A pan-HLA class I antibody was used to analyze HLA expression. This experiment was repeated four times with similar results. **b–d,** Comparison of percent of retics in RBC gate (b), percent of Retics that express HLA-I, (c) percent of SYBR $Green^+$ iRetics (d) in blood from HD (n=8) and Pv BT patients (n=8). Shown are mean ± SEM; statistical analysis by two-tailed non-parametric unpaired *t*-test at 95% CI. **e,** Comparison of HLA-ABC expression in circulating uRetics and iRetics in n=8 Pv BT samples, based on SYBR Green I and HLA staining of $CD235a^+CD71^+$ Retics, representative dot plot in (**a**). Shown are mean ± SEM; statistical analysis used a two-tailed parametric paired *t*-test at 95% CI. **f,g,** Comparison of HLA-ABC (**f**) and HLA-DR (**g**) expression by HD uRetics and Pv iRetics and $CD19^+$ B cells. Light gray histograms are unstained and darker gray histograms are stained cells. Shown are representative samples of 5 analyzed. **h,** Imaging flow cytometry of representative Pv uRetics (top) and iRetics (bottom) stained for CD235a, SYBR Green, CD71, HLA-ABC and HLA-DR. This experiment was repeated three times with similar results. **i,** Immunoblot of cell lysates from

3 HD uRetics and 3 Pv iRetics, loaded with 50 μg of protein per well and probed for the antigen processing protein, TAP1 as well as β-actin and F-actin as loading controls for HD uRetics and Pv BT iRetics, respectively. HD PBMCs were used as a positive control (20 μg). This experiment was repeated three times with similar results.

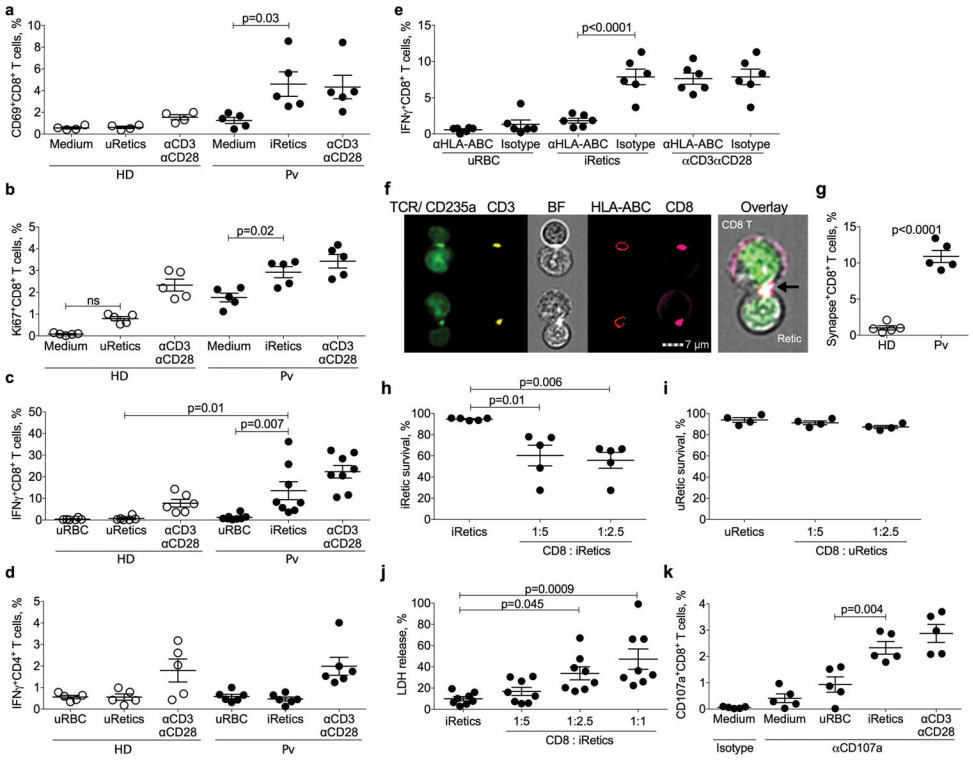

Figure 3. CD8$^+$ T cells are activated by and lyse autologous *P. vivax*-infected reticulocytes

a–d, Purified CD8$^+$ or CD4$^+$ T lymphocytes from healthy donors (HD) or *P. vivax* malaria patients (Pv) before treatment (BT) were cultured in medium alone, with autologous uninfected Retics (uRetics), with purified infected Retics (iRetics), or in the presence anti-CD3 and anti-CD28 and analyzed by flow cytometry for the proportion of CD8$^+$ T cells staining for CD69 (**a**) and Ki67 (**b**) (n=5) or intracellular IFNγ (**c**) (n=8); or CD4$^+$ T cells staining for intracellular IFNγ (**d**) (n=6). **e,** IFNγ expression by CD8$^+$ T cells after stimulation with autologous uninfected RBC (uRBC), purified iRetic or anti-CD3 and anti-CD28 in the presence of anti-HLA-ABC or isotype control antibody (n=6). **f,g,** Imaging flow cytometry analysis of immune synapse formation between CD8$^+$ T cells and autologous purified iRetics from Pv patients or uRetics from HD (n=5). Shown are representative images of immunological synapses between CD8$^+$ T cells and purified iRetics from a Pv sample (**f**) and mean ± SEM of the proportion of CD8$^+$ T cells forming synapses in 5 HD samples with autologous uRetics and in 5 Pv patient BT samples with purified iRetics (**g**). n=5 biologically independent samples/independent experiments. Cells were stained for TCR and CD235a, CD3, HLA-ABC, and CD8 and synapses were identified by the capping and co-localization of TCR, CD3, CD8 and HLA-ABC where the T cell and RBC are juxtaposed. The enlarged overlay image on the right corresponds to the bottom image. **h,i,** Survival of iRetics after 12 hr incubation with medium or autologous CD8$^+$ T cells from Pv samples (n=5) (**h**) or of uRetics incubated with medium or autologous HD CD8$^+$ T cells (n=4) (**i**), added at indicated E:T ratios, as assayed using CFSE-labeled Retics. **j,** iRetic lysis after 12 hr incubation with medium or autologous CD8$^+$ T cells from Pv samples (n=8), measured by LDH release. **k,** Frequency of CD8$^+$ T cells in the blood of 5 untreated Pv patients that degranulate, assessed by CD107a staining, in response to indicated

stimuli. Shown are mean ± SEM; statistical analysis by non-parametric two-way ANOVA (**a–e**), two-tailed non-parametric unpaired *t*-test at 95% CI (**g**), and non-parametric one-way ANOVA (**h–k**).

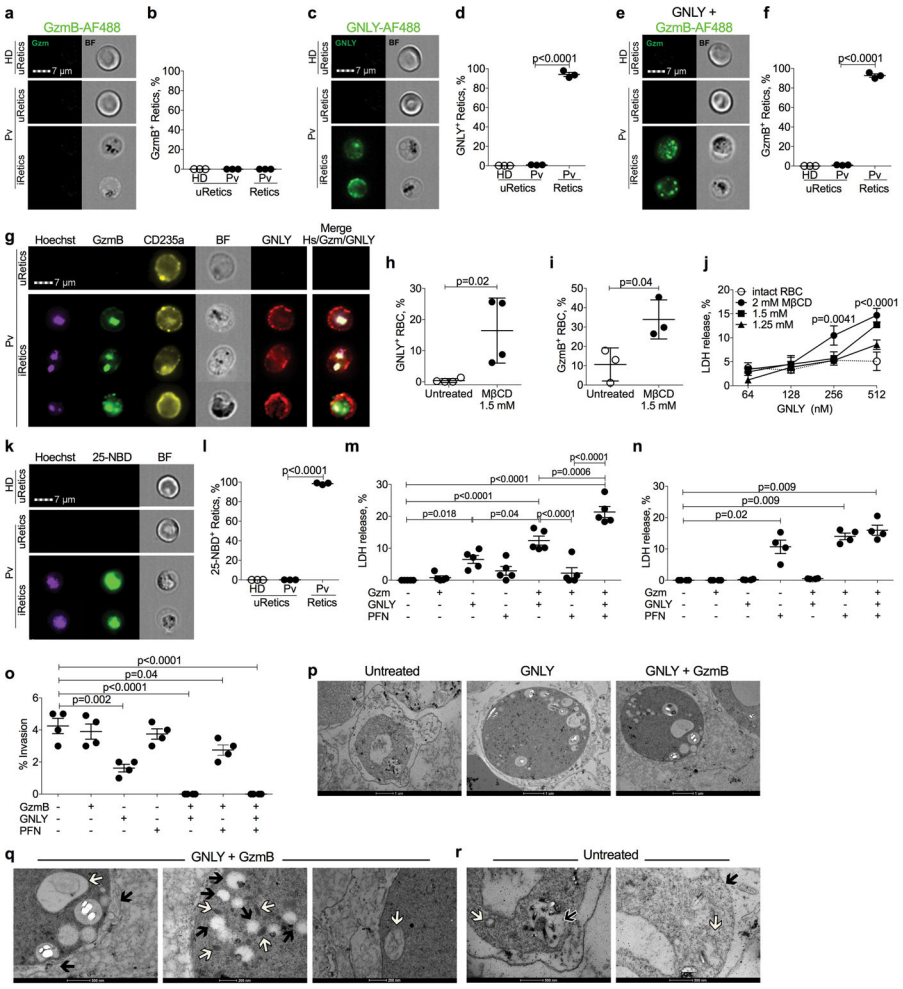

Figure 4. Granulysin binds to infected reticulocytes and mediates host cell lysis and parasite killing

a–f, Imaging flow cytometry analysis of uptake of GzmB-AF488 (**a,b**) or GNLY-AF488 (**c,d**) on their own, or of GzmB-AF488 in the presence of unlabeled GNLY (**e,f**) by healthy donor (HD) unifected Retics (uRetics) and by uRetics and infected retics (iRetics) from acute untreated *P. vivax* patients (Pv). (**a,c,e**) show representative images, while (**b,d,f**) show mean ± SEM of 3 HD and Pv samples. **g**, Imaging flow cytometry images of Pv uRetic and iRetics incubated with GzmB-AF488 and GNLY-AF750, and stained for CD235a and with a Hoechst dye to stain parasite DNA. BF, bright field. This experiment was repeated three times with similar results. **h–j,** Effect of mβCD depletion of cholesterol in HD RBCs on binding of GNLY-AF488 on its own (n=4). Shown p values are in comparison to intact RBC. (**h**) and of GzmB-AF488 in the presence of unlabeled GNLY (n=3) (**i**); and on RBC lysis by increasing amounts of GNLY, assessed by LHD release (n=4). **k,l,** Staining of HD uRetics and of untreated Pv patient uRetics and iRetics with the cholesterol analog 25-NBD (n=3). Representative images are shown in (**k**) (n=5) and the proportion of cells with detectable 25-NBD fluorescence is shown in (**l**) (n=4). **m,n,** Cytolysis of Pv iRetics (**m**, n=5) or HD uRetics (**n**, n=4) after 1 hr incubation with GzmB ± GNLY ± PFN, assessed by LDH release. **o,** Effect of incubation of iRetics from 4 Pv patients for 1 hr with indicated cytotoxic granule

proteins on parasite invasion of fresh Retics, assessed by Giemsa staining. **p–r,** Electron micrographs of iRetics that were untreated or incubated with GNLY ± GzmB. Higher magnification images after treatment with GNLY plus GzmB in (**q**) show parasitophorous vacuole membrane disruption (↑) and chromatin condensation (↟) (left); cytoplasmic vacuolization (↑) and dense granules (↟) (middle); and mitochondrial swelling (↟) (right). Higher magnification images of untreated cells (**r**) show intact digestive vacuole (↑), parasitophorous vacuole membrane (↑) and mitochondria (↟). These experiments were repeated three times with similar results (p,r). Graphs show mean ± SEM; statistics in (**b,d,f,j,l–o**) were analyzed by one-way ANOVA and in (**h,i**) by two-tailed non-parametric paired *t*-test at 95% CI.